Bioactive Materials 7 (2022) 181–191

Contents lists available at ScienceDirect

Bioactive Materials

journal homepage: www.sciencedirect.com/journal/bioactive-materials

High special surface area and "warm light" responsive ZnO: Synthesis mechanism, application and optimization

Xinxin Miao [a,1], Fen Yu [b,d,1], Kuan Liu [c], Zhongsheng Lv [c], Jianjian Deng [a], Tianlong Wu [a], Xinyan Cheng [b], Wei Zhang [b], Xigao Cheng [a,**], Xiaolei Wang [b,c,*]

[a] Department of Orthopaedic Surgery, The Second Affiliated Hospital of Nanchang University, Nanchang, Jiangxi, 330006, PR China
[b] College of Chemistry, NanChang University, NanChang, Jiangxi, 330031, PR China
[c] Institute of Translational Medicine, Nanchang University, Nanchang, Jiangxi, 330031, PR China
[d] Jiangxi Key Laboratory of Nanobiomaterials, Institute of Advanced Materials, East China Jiaotong University, Nanchang, Jiangxi, 330013, PR China

ARTICLE INFO

Keywords:
ZnO
Photocatalysis
Yellow light
Teeth whitening

ABSTRACT

In this study, a new series of zinc oxide (ZnO) with high specific surface area and narrow energy band gap are prepared using a facile microwave-induced method. The corresponding formation mechanism is also discussed for the first time. Due to the introduction of C, these ZnO can be excited by long wave temperature light without harmful short wave radiation, and play an efficient photocatalytic activity. This valuable property fundamentally improves the biological safety of its photocatalytic application. Herein, taking teeth whitening as an example, the photocatalytic performance of ZnO is evaluated. The "pure" yellow light-emitting diode (PYLED) with high biological safety is used as the excitation source. It is found that this method could effectively remove pigment on the tooth surface through physical adsorption. In addition, these ZnO could generate active oxygen to degrade the pigment on the tooth surface under the irradiation of yellow light. Some further optimization of these "warm light" responsive ZnO is also discussed in this systematical study, which could open up new opportunities in biomedical field.

1. Introduction

ZnO has attracted enormous attention for its unique chemical and physical properties [1–3]. As an important semiconductor material, ZnO exhibits excellent optical [4], magnetic [5,6], and piezoresistive properties [7], which has been widely used in catalysis [8,9], ceramics [10], sensors [11,12], and optoelectronic devices [13–15]. It's well known that ZnO has been approved by the U.S. Food and Drug Administration (FDA) as a material with good biocompatibility [16]. Therefore, ZnO also has extensive application prospects in biomedical field, including drug delivery [17], [[,18] imaging [19,20], implant materials [21,22] and biosensors [23,24]. Photocatalytic performance, as one of the research hotspots of ZnO, has laid a solid foundation for its application in environment and energy fields, but its application potential in the field of biomedicine has not been fully explored. What leads to this dilemma is that the traditional ZnO with wide energy band gap can only respond to short-wavelength light spectral region, such as ultraviolet light (UV light) [25–27]. In previous studies, some ZnO could be activated by visible light (purple light and blue light) through doping other metal elements, but new toxic substances may be introduced accordingly [28]. Besides, due to the hazards of short-wavelength light sources [29, 30], its application in biomedical area photocatalysis is severely restricted. Hence, it would be healthier if ZnO could be excited by some mild and long-wavelength visible lights (such as green, yellow or even red light). In other words, it's of great significance to effectively narrow the energy band gap of ZnO for improving the long-wavelength light response. In addition, the surface of existing ZnO is generally smooth and dense from the micron scale, which limited its adsorption capacity [31], and thus restricted the effects on environmental remediation or drug delivery [32] et al. Collectively, owing to the inherent poor visible light utilization and low specific surface area, their practical applications were greatly restricted, especially in biomedical field [33].

Peer review under responsibility of KeAi Communications Co., Ltd.
* Corresponding author. College of Chemistry, NanChang University, NanChang, Jiangxi, 330031, PR China.
** Corresponding author.
E-mail addresses: 228206846@qq.com (X. Cheng), wangxiaolei@ncu.edu.cn (X. Wang).
[1] These authors contributed equally to this work.

https://doi.org/10.1016/j.bioactmat.2021.05.027
Received 3 December 2020; Received in revised form 23 March 2021; Accepted 14 May 2021
Available online 31 May 2021

In this study, we developed a facile strategy assisted by a household microwave oven to synthesize a series of porous ZnO with long-wavelength warm light response and large surface area. The formation mechanism of its porosity was also investigated for the first time. Afterward, a safe long-wavelength yellow light was selected as the excitation light source, which has the characteristics of lower intensity and less irritation to the eyes [34,35]. The subsequent studies implied that, with the aid of yellow light, the synthesized ZnO could photocatalytic degrade pigments effectively. More importantly, owing to the peculiar healthier irradiation activated capability, its photocatalytic application would be no longer limited to the environmental field. As a proof of concept study, taking teeth whitening as an example, the expanded applications of ZnO in biomedical field was demonstrated.

2. Materials and methods

2.1. Materials

$Zn(NO_3)_2{\cdot}6H_2O$, hexamethylenetetramine (HMT), sodium citrate, and hydroxypropyl methyl cellulose (HPMC) were purchased from Macklin (Shanghai, China). Rhodamine B (RhB) for photocatalytic degradation was purchased from Sinopharm Chemical Reagent Co. Ltd. (Shanghai, China). Roswell Park Memorial Institute (RPMI) 1640 medium, fetal bovine serum (FBS), and penicillin streptomycin were supplied by Gibco Co. (USA). Cell counting assay kit-8 (CCK-8) was purchased from Dojindo Co. (Japan).

2.2. Preparation of PZCs

50 mM $Zn(NO_3)_2{\cdot}6H_2O$, 80 mM $NH_3{\cdot}H_2O$ and 25 mM HMT were dissolved in 400 mL deionized water by stirring for 10 min in a sealed container. Then the reaction system was put into a water bath at 65 °C for 15 min. After that, 0.14 g sodium citrate and 0.1 g HPMC were added to the solution under magnetic stirring until a homogeneous solution was formed. The mixed solution was incubated for 10 h in a water bath at 85 °C. After the reaction, the product was collected by centrifugation and washed twice with deionized water and ethyl alcohol, and finally dried in the vacuum freezer dryer. After freeze drying, PZCs were obtained with microwave treatment for 15 min.

2.3. Preparation of BC

Firstly, 100 g wheat-straws were washed with deionized water and dried in an oven for 24 h. Then these wheat-straws were cut into small segments (3.8 cm). Subsequently, calcination was carried out under a nitrogen atmosphere in a tubular furnace at 800 °C for 1 h with a heating rate of 5 °C/min. After that, the tubular furnace was cooled to 300 °C at the rate of 5 °C/min, and then naturally cooled to room temperature. Finally, the biomass carbon (BC) was obtained after washing with deionized water and drying at 80 °C in the oven for 12 h.

2.4. Preparation of ZnO-BC 1

$ZnNO_3{\cdot}6H_2O$ (0.7437 g) was dissolved in deionized water (50 mL). Under the constant stirring, 50 mL NaOH solution (0.05 mol/L) was added to the $ZnNO_3{\cdot}6H_2O$ solution at room temperature to form Zn $(OH)_2$ colloid. The obtained colloidal solution was then centrifuged for 10 min at 8000 rpm, and the supernatants were discarded. Subsequently, the precipitate and BC (0.1 g) were dispersed in 50 mL H_2O_2 solution (1 mol/L). Then, the solution was transferred into an oven and dried at 75 °C for 24 h. The dried sample was put into the tube furnace and calcined at 1000 °C for 2 h under a nitrogen atmosphere. Finally, the ZnO-BC 1 was obtained.

2.5. Preparation of ZnO-BC 2 and ZnO-BC 3

50 mM $Zn(NO_3)_2{\cdot}6H_2O$, 80 mM $NH_3{\cdot}H_2O$ and 25 mM HMT were dissolved in 400 mL deionized water by stirring for 10 min in sealed. Then the reaction system was put into a water bath at 65 °C for 15 min. After that, 0.14 g sodium citrate, 0.1 g HPMC and 0.1 g BC were added to the solution under magnetic stirring until a homogeneous solution was formed. The mixed solution was incubated for 10 h in a water bath at 85 °C. After the reaction, the product was collected by centrifugation and washed twice with water and ethyl alcohol. Finally, the ZnO-BC 2 was obtained after freeze drying. ZnO-BC 3 was obtained by microwave treatment of ZnO-BC 2 for 15 min.

2.6. Visible light photocatalysis

The photocatalytic activities of these samples were evaluated by the degradation of RhB at room temperature. The reaction systems were stirred under the visible light condition (blue, yellow, green and white light). The visible light photocatalytic activity was tested by a wavelength scan on a UV–vis spectrophotometer.

2.7. Absorption of Cu^{2+}

$CuCl_2{\cdot}2H_2O$ was dissolved in deionized water. Then five kinds of ZnO samples (0 min, 1 min, 3 min, 5 min, 15 min) were added to the solution, respectively. After 2 h, the content of residual Cu in the solution was measured by inductively coupled plasma spectroscopy (ICP).

2.8. Teeth whitening

Teeth were obtained from the Affiliated Dental Hospital of Nanchang University. The PYLED chip was installed in the head of the toothbrush. The teeth were immersed in the solution of samples (5 mg/mL), and brushed with the PYLED-toothbrush under the irradiation of PYLED for 0.5 h. Finally, the dental professional color card was used to evaluate the whitening effect.

2.9. Residual bacterial on teeth

We selected three groups of teeth possessed the same size to conduct the experiment. After the teeth were washed, they were sterilized by autoclave. Then, the three groups teeth and bacterial solutions (*S. aureus*, *E. coli*) were placed in a biochemical constant temperature incubator (37 °C, 120 rpm/min) for 24 h. The teeth of group 1 were brushed with toothbrush as control, the teeth of group 2 were brushed with sample, the teeth of group 3 were brushed with sample under PYLED irradiation, and each group of teeth was brushed for 3 min. Then three groups of teeth were washed twice with PBS. Finally, the SEM images of naturally air-dried teeth were taken to observe the bacteria remaining on the surface of the teeth.

2.10. Statistical analysis

Data were represented as means ± standard deviation (SD). Statistical analyses were performed using GraphPad Prism (GraphPad Software, Inc., San Diego, CA). Data were analyzed using one-way analysis of variance (ANOVA) and unpaired or paired Student's *t*-test as appropriate. Significance was accepted at $p < 0.05$.

All experiments were performed in compliance with the relevant laws and approved by the Institutional Animal Care and Use Committee at Institute of Translational Medicine, Nanchang University.

3. Results and discussion

3.1. Synthesis and characterization of PZCs

Firstly, we synthesized porous ZnO capsules (PZCs) through a simple household microwave process, as shown in Fig. 1a. The precursor of PZCs was synthesized by a water bath method. After freeze drying, a facile microwave treatment was carried out. Through scanning electron microscope (SEM) observation, the morphology of original ZnO was nanosheet. During the process of microwave, these nanosheets gradually agglomerated into microspheres, and finally formed PZCs after 15 min (Fig. 1b–f). Transmission electron microscope (TEM) analysis further confirmed the morphological changes of ZnO under different microwave time treatments (Fig. 1g–i). High resolution TEM (HRTEM) images and selected area electron diffraction (SAED) patterns also implied that, when the microwave time reached 15 min, the crystal structure of the ZnO was changed from single crystal to polycrystal (Fig. S1). The polycrystalline structure was mainly due to the introduction of carbon into ZnO after the carbonization of hydroxy propyl methyl cellulose (HPMC), and eventually C-doped PZCs were synthesized.

Subsequently, the influence of microwave power on the morphology of ZnO was studied. SEM images exhibited that the porous structure could be formed only when the microwave power reached 100% (800 W) (Fig. 2a–d). The element analysis implied that the contents of two elements (Zn and O) basically kept unchanged after microwave treatment (Fig. 2e and f).

The X-ray diffraction (XRD) patterns (Fig. 2g) with prominent peaks along (101) and (103) showed the polycrystalline nature of these ZnO. Besides, characteristic peaks of $Zn(OH)_2$ could also be observed from the diagram, indicating the presence of $Zn(OH)_2$ in the early stage of ZnO synthesis. With the increase of microwave time, $Zn(OH)_2$ was gradually decomposed into ZnO. Through X-ray photoelectron spectroscopy (XPS) spectrogram analysis, when the microwave time reached 15 min, there were little $Zn(OH)_2$ in sample (Fig. S2), which was consistent with previous results. Furthermore, thermal stabilities of ZnO were studied using the thermogravimetric analysis (TG). As a result, all kinds of ZnO showed a similar degradation trend, and the degradation process was governed by two stages (Fig. 2h). In the first stage, the weight loss occurred in the range of 25 °C–175 °C, which was mainly due to the removal of weakly adsorbed water on the surface of ZnO. The second weight loss step, which occurred above 250 °C, was mainly owing to the decomposition of crystal water and $Zn(OH)_2$ and the carbonization of HPMC. Fourier transform infrared spectroscopy (FTIR) was subsequently utilized to analyze the structural changes of samples after different microwave time treatments (Fig. 2i). The results confirmed the presence of –OH on the surface of all kinds of ZnO. The peak at 3328 cm^{-1} was attributed to the vibration of –OH, which was obviously decreased with prolong of microwave time. To sum up, the formation mechanism of PZCs in the microwave process was simply summarized in Fig. S3. As the microwave pyrolysis proceeded, the generated water vapor and carbon dioxide (CO_2) generated by the carbonization of HPMC escape from the surface of the ZnO microspheres, forming irregular pores on the surface of ZnO microspheres.

3.2. Adsorption and photocatalytic activities of PZCs

To further validate the porous structure, the adsorptive experiment of cupric ion (Cu^{2+}) was performed. The results showed that PZCs (15 min) exhibited the highest adsorptive capacity compared with others (Fig. 2j). Subsequently, the porous property of the PZCs was also investigated by nitrogen adsorption. According to the nitrogen adsorption-desorption isotherms (Fig. 2k), PZCs (15 min) possessed a specific surface area of 59.784 m^2/g, which was higher than that of ZnO without microwave treatment (0 min). Meanwhile, PZCs had an average pore size of 30.798 nm and a total pore volume of 0.153 cm^3/g (Fig. S4). In addition, the methanol adsorption results also proved that PZCs (15 min) had the stronger adsorptive capacity than ZnO without microwave treatment (0 min) (Fig. S5).

Next, their photocatalytic performances were studied. Firstly, the photocatalytic efficiencies of these ZnO were evaluated by degradation experiments using Rhodamine B (RhB). As illustrated in Figure 2l, the photocatalytic activities of all kinds of ZnO were significantly enhanced by treating with microwave. Furthermore, the degradation efficiency of RhB showed a positive correlation with microwave time. According to the degradation results of RhB, three kinds of ZnO (0 min, 5 min and 15 min) were selected for further research. Subsequently, through the calculation of their ultraviolet–visible (UV–vis) spectra, the optical energy band gaps of these three kinds of ZnO were 3.25 eV for 0 min, 3.18

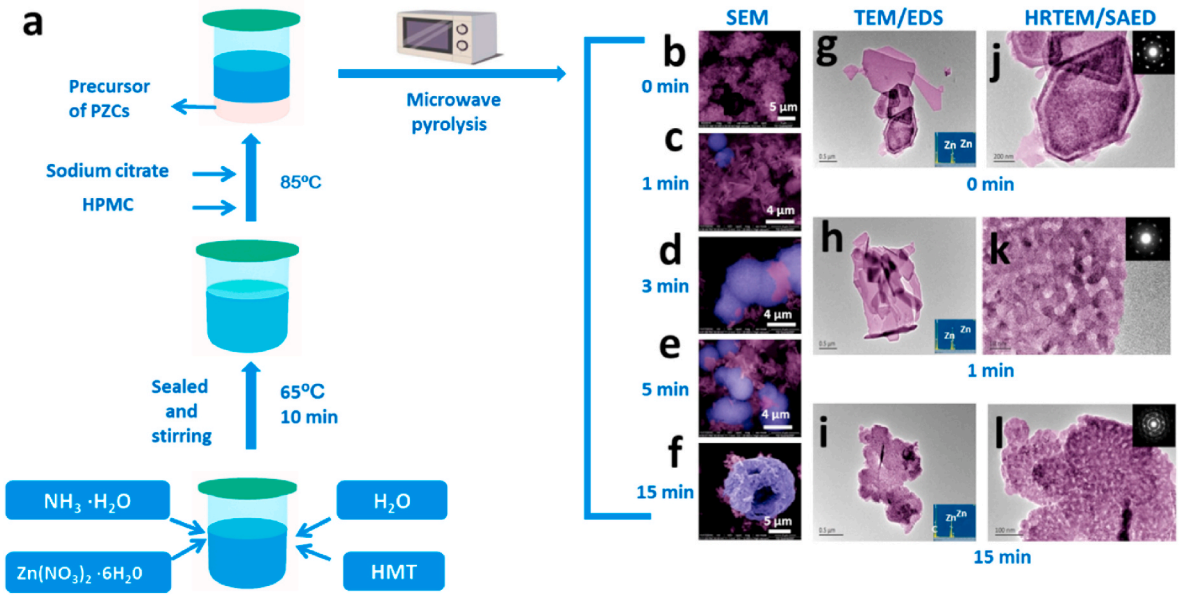

Fig. 1. Schematic illustration of the synthetic route for preparing PZCs. (a) Schematic illustration for the synthesis of PZCs precursor. (b–f) SEM images of ZnO after treatment with microwave at different time points. (g–i) TEM images and (j–l) HRTEM images of ZnO after treatment with microwave at different time points. Insets in g-i are the corresponding images of EDS, and j-l are the corresponding SAED patterns.

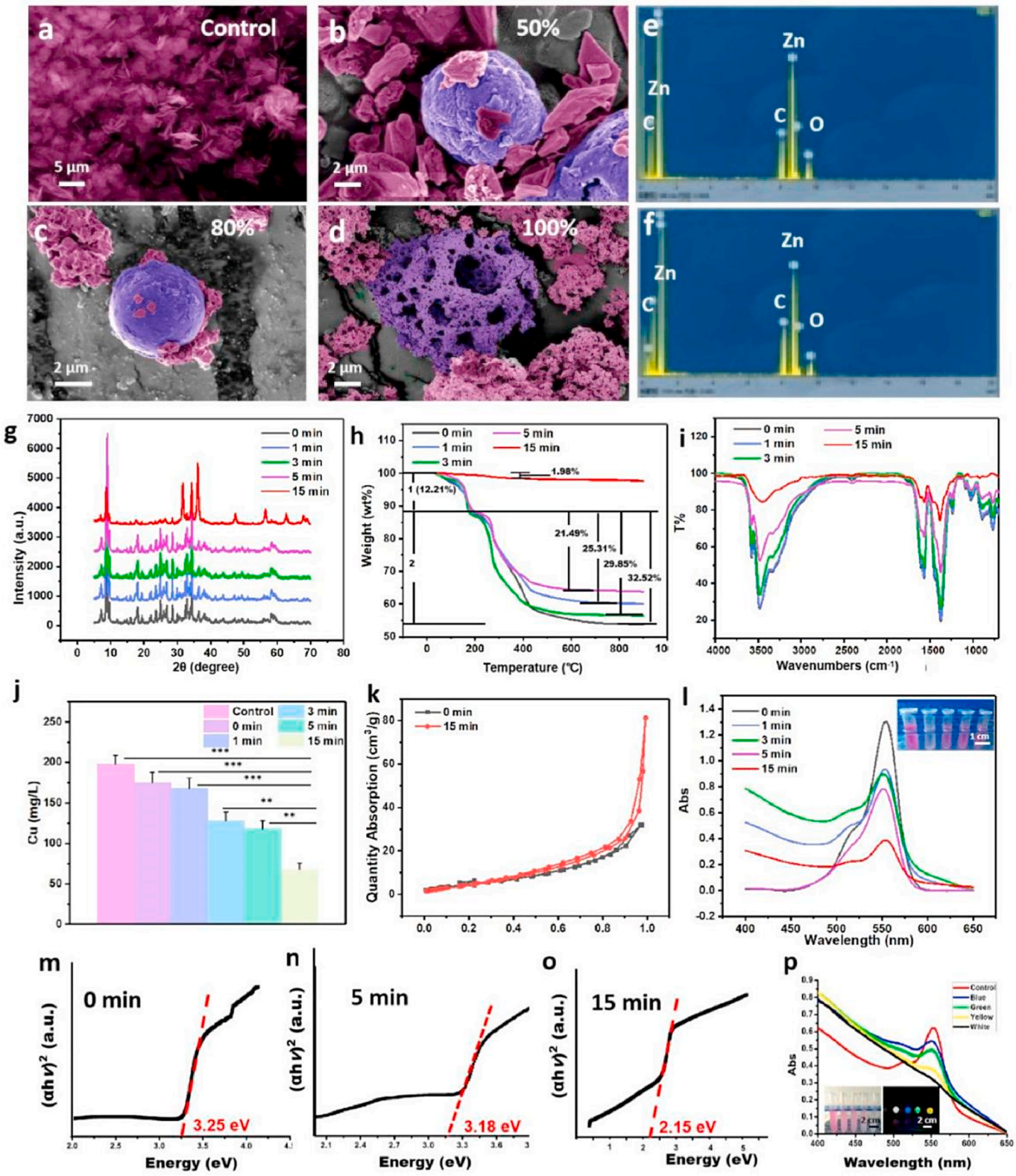

Fig. 2. Characterization of PZCs. (a–d) SEM images of ZnO after treatment with different microwave power. ZnO without microwave treatment was used as the control group. 100% power was 800 W, and 80% power was 640 W, 50% power was 400 W. (e, f) Corresponding EDS of ZnO without microwave treatment (e) and PZCs (f). (g) XRD patterns of ZnO after treatment with microwave at different time points. (h) TG curves of ZnO after treatment with microwave at different time points. (i) FTIR spectra of ZnO after treatment with microwave at different time points. (j) Residual Cu concentrations after treatment with different ZnO. Date are mean ± SD. n = 3. *$p < 0.05$, **$p < 0.01$, ***$p < 0.001$. (k) Nitrogen adsorption-desorption isotherm curves of ZnO without microwave treatment (0 min) and PZCs (15 min). (l) UV–vis absorption spectra of RhB at different time points under UV light. The inset is the optical photograph of RhB degradation efficiency. (m–o) $(\alpha Ep)^{1/2}$ *vs* Ep plots of ZnO. (p) Photocatalytic effects of RhB after treatment with PZCs under different visible light sources irradiation. Natural light was used as the control group. The insets are the optical photograph of RhB degradation efficiency and the optical photograph of RhB degradation process using different light sources, respectively.

eV for 5 min and 2.2 eV for 15 min (PZCs) (Fig. 2m–o). The results indicated that energy band gaps were decreased with the increase of microwave time. The narrower energy band gap of PZCs meant that the photocatalytic reaction could be triggered under a long-wavelength visible light condition. The reason for this phenomenon may be that there is an empty orbital on the 2p sublayer orbital of C. The hybridization of the empty orbital state with the 2p orbital electronic energy state of O leads to the energy level structure between ZnO lattices, which reduces the band gap and realizes the absorption of visible light. Moreover, according to photoluminescence (PL) spectra (Fig. S6), with the introduction of C, there are impurity energy levels, oxygen vacancies, interstitial zinc, zinc vacancies and interstitial oxygen energy levels in ZnO lattice. These energy levels will form new recombination centers and cause the change of band gap. With the introduction of C, the near band edge emission peak of C-doped ZnO shifts to red, which indicates that C-doping can effectively reduce the optical band gap of ZnO.

To further verify this phenomenon, PZCs were chosen as the photocatalysts to degrade RhB under different visible light conditions with consistent intensity. Herein, four kinds of representative visible light sources were selected, including blue, green, yellow and white light. The results showed that yellow light exhibited the best degradation performance (Figure 2p), except white light (because white light is a mixed light composed of blue, red and green light in a certain proportion [36]). Moreover, reusability studies were performed to check the recyclability of PZCs. As Fig. S7 showed, although some porous structures of recovered PZCs collapsed, the degradation efficiency was not significantly affected, which proved the good reusability of PZCs.

3.3. Application in teeth whitening

According to above results, one of the important highlights of PZCs was that they could be excited by long-wavelength visible light. Yellow light is a low color temperature light source, namely warm light. In previous studies, our research group have developed a high-efficiency "pure" yellow light-emitting diode (PYLED, 1900 K, without blue light spectrum, Fig. S8) and proved its good biocompatibility [37]. In recent years, with the development of biomedical technology, people's requirements for teeth no longer stayed on the absence of dental disease. Instead, healthy and white teeth have been regarded as one of the criteria for beauty. Under the circumstances, teeth whitening has become one of the focus items [38]. At present, "cold light whitening" is the most commonly used method [39,40]. This method mainly uses high-intensity blue light with a wavelength of 480 nm–520 nm to irradiate the reagent containing hydrogen peroxide (H_2O_2) as the main component. Under the irradiation of blue light, the reagent would produce an oxidation-reduction reaction with the pigments attached to the surface or deeper layer of teeth, finally achieved the whitening effect. Although this method has shown good whitening effects, there are still some inevitably side effects such as enamel demineralization, soft tissue stimulation and tooth sensitivity [41]. Besides, the long-term strong irritation of blue light to the eyes may cause damage to the lens of users [42]. In this case, it would be expected to improve the safety of such method if there was a whitening reagent which could be catalyzed by a mild light source. Based on this requirement, PZCs, which possessed two characteristics of adsorptive capability and visible light catalysis, were used for teeth whitening as an example of their biomedical application. Compared with "cold light whitening", a long-wavelength warm light with higher safety was selected here as the light source, and we named this method "warm light whitening".

With the aid of a customized mini PYLED chip, a yellow light-emitting brush was designed and made (Fig. 3a). Then, the experiments of "warm light whitening" were conducted using this self-made brush and PZCs. The results showed that PZCs under PYLED irradiation had a certain whitening effect on teeth (Fig. 3b–d). The mechanism of this whitening method could be summed up as follows. The first one was that under PYLED irradiation, PZCs could produce reactive oxygen species (ROS) to induce the oxidation-reduction reaction. Then the pigments around the teeth were degraded, so as to achieve the goal of teeth whitening. The other was the adsorptive action. We have previously demonstrated that the PZCs are porous, so they could also achieve the effect of teeth whitening by adsorbing pigments. Moreover, the SEM images exhibited that PZCs had no obvious damage to tooth enamel, even after treatment for a long time (0.5 h). As a comparison, when treated with the dental used H_2O_2, the tooth enamel was severely damaged (Fig. 3e–j). These results demonstrated that PZCs combined with PYLED was a safe and effective method for teeth whitening.

Then we further verified whether the PYLED irradiation could improve the whitening effect of PZCs. The results were illustrated in Fig. 3k-r. It could be observed that the whitening effect of PZCs combined with PYLED irradiation was better than that of PZCs alone (Fig. 3k-n). Commercial tooth-paste was used as the control. Because the tooth-paste did not contain any components that could be excited by visible light, the irradiation of PYLED had little effect on it (Fig. 3o–r). Meanwhile, according to the dental professional color card, the whitening effect of PZCs was much better than that of tooth-paste under the same condition (Fig. S9). On this basis, we investigated whether the changes in output voltage and current would affect the whitening effect of PYLED. Herein, different output voltages and currents were used to test whether they would affect the whitening effect of PYLED. As shown in Fig. S10, under the same condition, there was no significant influence on the whitening effect by increasing the output voltage or current. In other words, we just need a low-power portable light-emitting toothbrush and PZCs, the purpose of teeth whitening would be achieved easily.

3.4. Antibacterial properties and cytocompatibility of PZCs in vitro

Bacteria on the surface of teeth would have a significant impact on oral health. Dental plaque and periodontitis caused by incomplete teeth brushing may increase the risk of cancer death [43]. It's well known that Zn is an essential trace element in the human body, and ZnO is an inorganic material with good antibacterial property and biocompatibility [44,45]. In this study, we also researched the antibacterial ability of PZCs. As shown in Fig. 3s-t, tooth-paste had almost no antibacterial activity, while PZCs exhibited excellent antibacterial properties against gram-positive (*S. aureus*, Fig. 3s) and gram-negative bacteria (*E. coli*, Figure 3t) (Fig. S11). Meanwhile, the residual bacteria on the surface of teeth after treatment with PZCs were decreased significantly (Fig. 3u–x). To assess the biocompatibility of PZCs, mice were given PZCs by oral gavage for 10 d and the hematoxylin and eosin (H&E) staining analysis was conducted subsequently. During oral gavage with PZCs, these mice did not suffer diarrhoea or weight loss (Fig. S12). Beyond that, the results of H&E staining revealed that there were no remarkable tissue damages or any significant side effects on heart, liver, spleen, lung, kidney (Figure 3y). Furthermore, the results of the cell viability *in vitro* demonstrated the PZCs possessed good cell compatibility (Fig. S13). Moreover, the morphology of human umbilical vein endothelial cells (HUVECs) was observed by fluorescence microscope. As shown in Fig. S14, there were no significant changes in the morphology of HUVECs. Taken together, all above results suggested PZCs had good biocompatibility. To sum up, "warm light whitening" had a great application prospect in teeth whitening and oral hygiene in the future.

3.5. Synthesis and characterization of ZnO-BC

Considering that the limited increase of specific surface area of PZCs over traditional ZnO, which meant the adsorptive capacity of PZCs for pigment was restricted to some extent. Again, we hope to further improve the warm light response characteristics of ZnO and make it have narrower energy band gap. Therefore, it was of great significance to further improve the adsorptive capacity of material for teeth

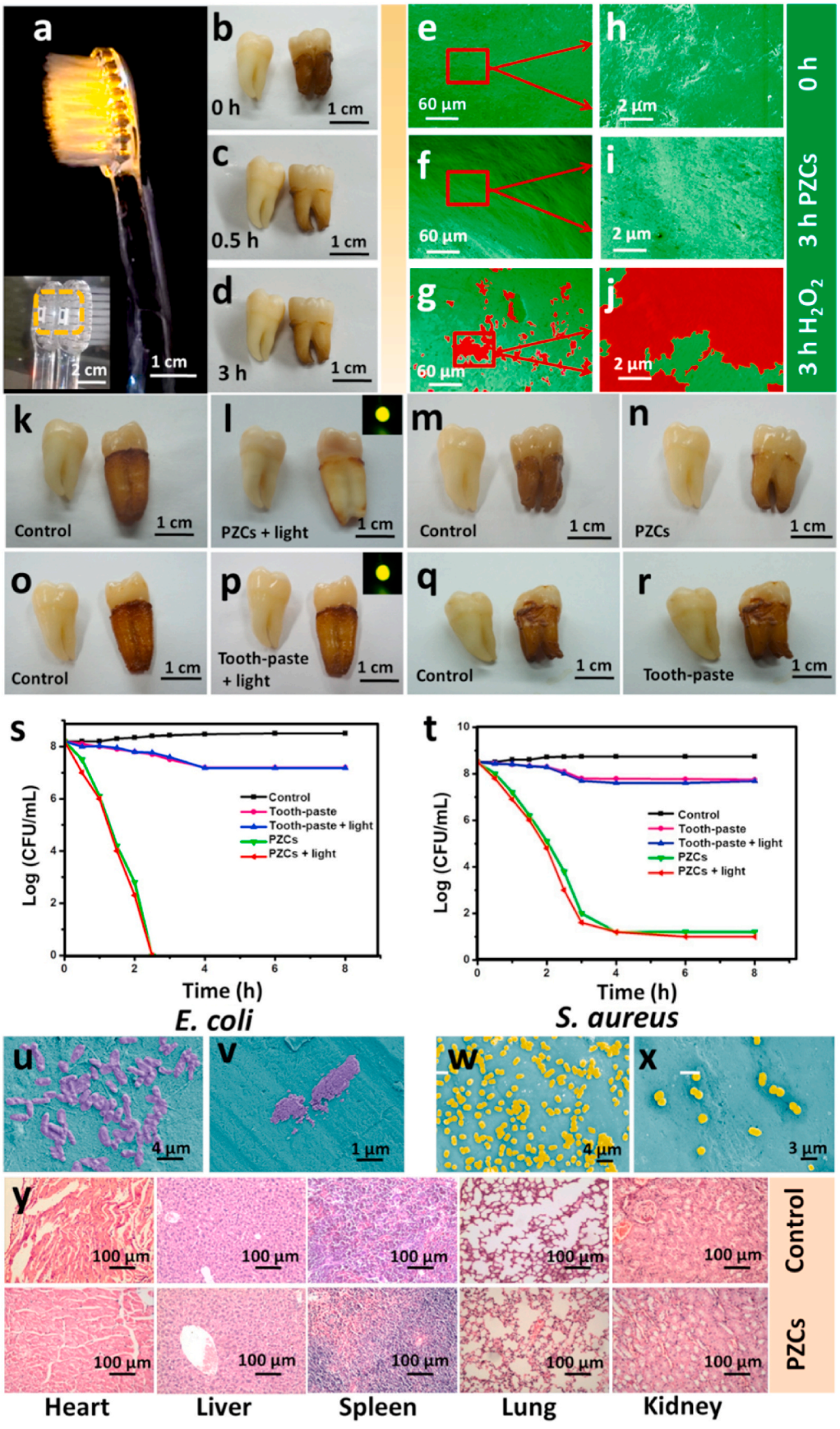

Fig. 3. Teeth whitening. (a) The optical image of the self-made PYLED-toothbrush. The inset is the optical photograph of the back of the toothbrush, and the location of the built-in PYLED chip was marked with yellow box. (b–d) Optical photographs of teeth after whitening treatment with different time. No treatment was done in the control group. (e–j) SEM images of tooth enamel without any treatment (e), and after treatment with PZCs (f), H_2O_2 (g) for 3 h, respectively. Green: normal tooth enamel, red: damaged tooth enamel. (h–i) Enlarged images of e-g. (k–r) Optical images of teeth treated with different whitening methods. In order to compare the whitening effect of teeth, the left teeth were used as the control. No treatment was done in the control group. (s, t) The antibacterial activity against *S. aureus* (s) and *E. coli* (t). No treatment was done in the control group. (u–x) SEM images of *E. coli* (u, v) and *S. aureus* (w, x) on the surface of teeth after whitening treatment with PZCs. (y) The H&E staining images of heart, liver, spleen, lung and kidney after treatment with normal saline (control) and PZCs on day 10.

whitening. Owing to its excellent adsorption performance and chemical stability, activated carbon (AC) has been widely used to remove organic contaminants from waste water [46,47]. If the photocatalytic performance of ZnO could be combined with the high specific surface area of AC, the whitening effect of teeth might be considerably improved. Therefore, further improvements were made in synthesis method to obtain ZnO with these properties, so as to achieve the purpose of more effective adsorption and degradation performance.

In the following study, as shown in Fig. 4a, biochar (BC) was first fabricated using wheat-straw (a common natural AC source), and accordingly synthesized three kinds of composites of ZnO and BC (ZnO-BC). The SEM images of three kinds of ZnO-BC indicated that ZnO was successfully loaded on the surface of BC (Fig. 4b). The XRD patterns confirmed that there were characteristic peaks of C and ZnO in three kinds of ZnO-BC (Fig. 4c). Their element distribution maps, TEM and SAED images proved the distribution of ZnO on the surface of BC (Fig. S15, Fig. S16). The XPS spectra of three kinds of ZnO-BC revealed the presence of C, O and Zn (Fig. S17). In the FTIR spectra, because both ZnO-BC 1 and ZnO-BC 3 were subjected to a high-temperature treatment, the intensity of –OH at 3328 cm^{-1} was lower than that of ZnO-BC 2 (Fig. 4d). In the TG diagram, ZnO-BC 1 and ZnO-BC 3 also exhibited similar pyrolysis processes (Fig. S18). Moreover, during the research, we found that three kinds of ZnO-BC had near-infrared photothermal effects (Fig. S19).

3.6. Adsorption and photocatalytic activities of ZnO-BC

It can be seen from previous studies that adsorption and photocatalysis were two major factors affecting the whitening effect of teeth. Focusing on these two characteristics, three kinds of ZnO-BC were further studied. According to the nitrogen adsorption-desorption isotherms, ZnO-BC 3 possessed the highest specific surface area, which was about 313.47 m^2/g (Fig. 4e). Then their photocatalytic performances were characterized by UV–vis absorption spectroscopy. As can be seen from Fig. 4f, the energy band gap of ZnO-BC 3 was the narrowest, only 1.9 eV. Compared with PZCs, ZnO-BC 3 could respond to a wider range of visible light. Subsequently, we also investigated their photocatalytic performances under PYLED condition. According to the results of photocatalytic degradation of RhB (Fig. 4g), ZnO-BC 3 had the best degradation performance, and the degradation rate could reach 87.78% after 10 min (Fig. S20a). It's worth noting that ZnO-BC 2 could only be excited by UV light in theory due to the wide energy band gap (3.2 eV), and theoretically they should have little degradation effect under PYLED irradiation. However, from the results, ZnO-BC 2 still reduced the UV absorption peak of RhB under PYLED irradiation (Fig. 4g). This phenomenon was mainly attributed to the adsorption of ZnO-BC 2. Meanwhile, although ZnO-BC 1 could also be excited by PYLED, their degradation effects were obviously lower than that of ZnO-BC 3 (Fig. S20b). The reason was that compared with ZnO-BC 3, ZnO-BC 1 possessed a lower specific surface area and a wider energy band gap.

3.7. Application in "warm light whitening"

Based on the above results, these three kinds of ZnO-BC were applied to the "warm light whitening" experiments, as shown in Fig. 5a. According to the dental professional color card (Fig. 5b), it could be seen that teeth were only whiter for 1 color gradation after brushing with tooth-paste (Fig. 5c). Surprisingly, it was found that teeth were whiter for 13 color gradation after brushing with ZnO-BC 3 for 0.5 h under the irradiation of PYLED. Although the other two ZnO-BC also improved the color gradation to a certain extent, their whitening effects were obviously lower than that of ZnO-BC 3. Subsequently, the surfaces of teeth were clearly observed by SEM. As displayed in Fig. 5d, H_2O_2 caused serious damage to tooth enamel, while there were no obvious damages after treating with three kinds of ZnO-BC. Furthermore, the antibacterial properties of these three kinds of ZnO-BC were evaluated by calculating the bacterial survival rate. It was found that the antibacterial activity of ZnO-BC 3 was the best (Fig. S21). Afterward, the reduction of bacteria adhering to the teeth surface was clearly observed by SEM images (Fig. 5e and f).

3.8. Biocompatibility of ZnO-BC

To estimate the biocompatibility of these three kinds of ZnO-BC, *in vitro* experiments were carried out by co-culturing with HUVECs. Then the Cell Counting Kit-8 (CCK-8) was used to determine cell viability and a concentration-dependent decrease in cell survival was observed (Fig. S22). After 7 d, all three kinds of ZnO-BC had certain promotion effects on cells. Moreover, there were no significant changes in cell morphology (Fig. S23). In order to further verify their biosafety *in vivo*, mice were respectively given three kinds of ZnO-BC by oral gavage for 7 d and their body weight changes were recorded every day. The results showed there were no obvious impacts on mice weight (Fig. S24). After this experiment, these mice were sacrificed, and their hearts, livers, spleens, lungs, and kidneys were taken for H&E staining, and the toxic side effects of ZnO-BC on them were analyzed. From the results of H&E staining, no significant inflammations and injuries were found in the tissues of the experimental group (Fig. S25). In sum, all the evaluations demonstrated that ZnO-BC had good biocompatibility. In the course of this study, we accidently found that ZnO-BC 3 could be slowly dissolved in saliva (Fig. S26), and the hemolytic rate was less than 2% after pigment degradation (Fig. S27). This phenomenon indicated that even if there were residual ZnO-BC 3 in the oral cavity, they would be gradually dissolved in saliva and would cause limited impact on health. Based on all above results, it can be concluded that "warm light" assisted ZnO-BC was a safe and effective method for teeth whitening.

4. Conclusion

In summary, a new series of ZnO with high specific surface area and narrow energy band gap were obtained by microwave-induced method. Although the specific surface area of PZCs was improved compared with traditional ZnO, there were some limitations in adsorption. In order to obtain those ZnO with the high specific surface area characteristic of AC and the narrow energy band gap characteristic of PZCs, our experimental scheme was further improved, and finally ZnO-BC composites with these characteristics were synthesized. These valuable characteristics, we believe that these capabilities make the photocatalytic application of ZnO no longer restricted to the environment and energy fields, and they also have wider potential in the biomedical field. In this study, we chose teeth whitening as an attempt. Combined with the irradiation of PYLED, the prepared ZnO-BC 3 had the best whitening effect through adsorbing and degrading pigments attached on the surface of teeth. Furthermore, owing to the good antibacterial property, they can effectively kill oral pathogens. Based on these characteristics, the concept of "warm light whitening" was first demonstrated. Compared with "cold light whitening", this method had the advantages of reducing the irritation to the teeth from both the light source and oxidizing material while ensuing the whitening effect. The emergence of "warm light whitening" means that teeth whitening technology would bid farewell to sensitivity and irritation, and enter the era of "warm and comfortable" enjoyment. It is worth noting that during the optimization process, we found that with the amount of BC increasing, the long-wavelength warm light response ability and the adsorption effect of ZnO-BC were improved. Furthermore, the incorporation of BC endowed them with stronger near-infrared photothermal effects, which was expected to be used to regulate drug release and target thermotherapy. However, we also found that excessive amounts of BC may cause some cytotoxicity. Therefore, we hope to further improve their biosafety through surface modification technology, and extend the concept of "warm light" photocatalysis to more biomedical applications in the future.

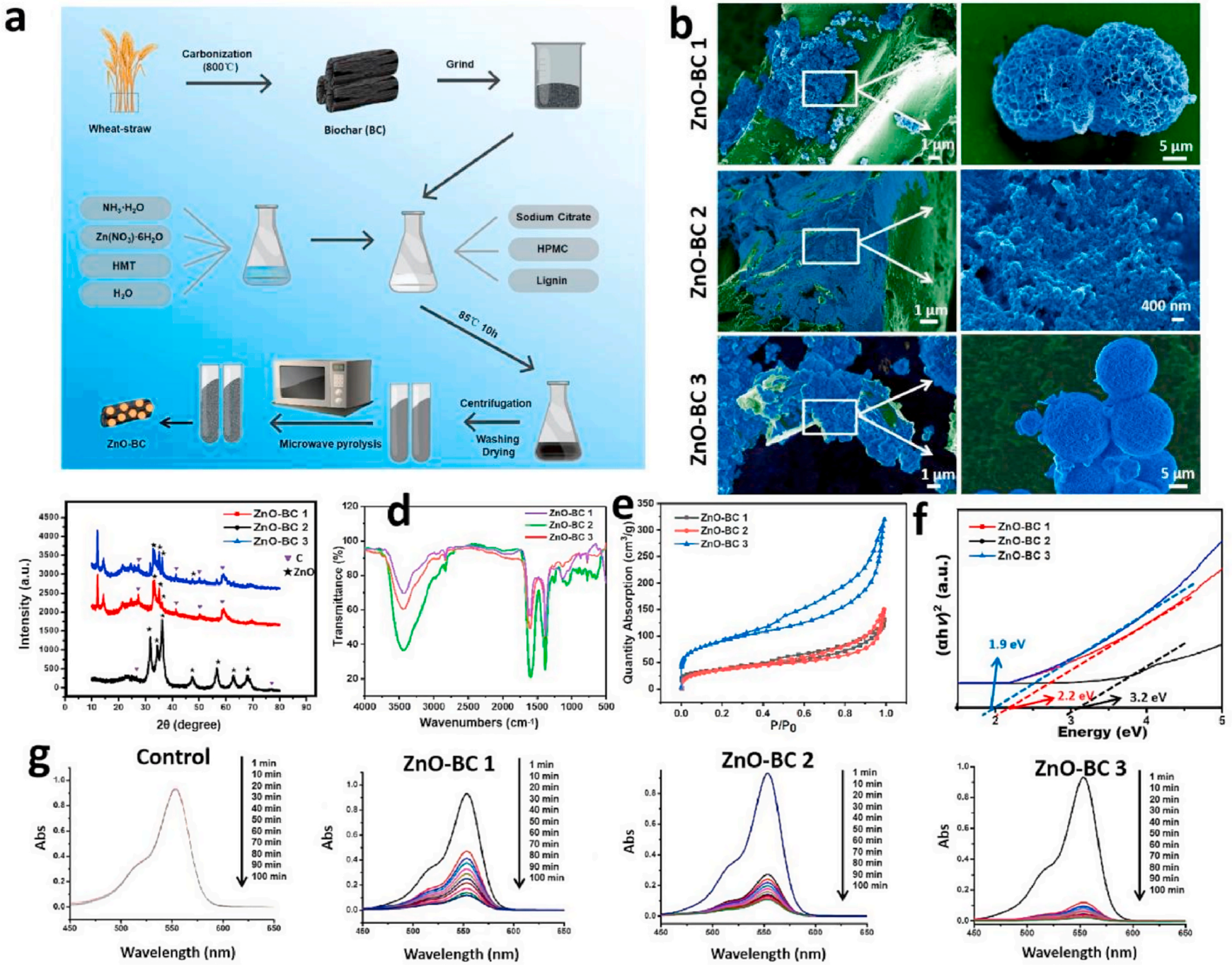

Fig. 4. Characterization of ZnO-BC. (a) Schematic illustration for the synthesis of ZnO-BC. (b) SEM images of three kinds of ZnO-BC. Images on the right are larger versions of ZnO loaded on the surface of BC. Green: BC. Blue: ZnO. (c–d) XRD patterns and FTIR spectra of ZnO-BC 1, ZnO-BC 2 and ZnO-BC 3. (e) Nitrogen adsorption-desorption isotherm curves of ZnO-BC 1, ZnO-BC 2 and ZnO-BC 3. (f) $(\alpha\ Ep)^{1/2}$ *vs* Ep plots of three kinds of ZnO-BC used to determine their optical band gap energy levels. (g) UV–vis absorption spectra of RhB after treatment with ZnO-BC 1, ZnO-BC 2 and ZnO-BC 3 at different time points under PYLED irradiation. No treatment was done in the control group.

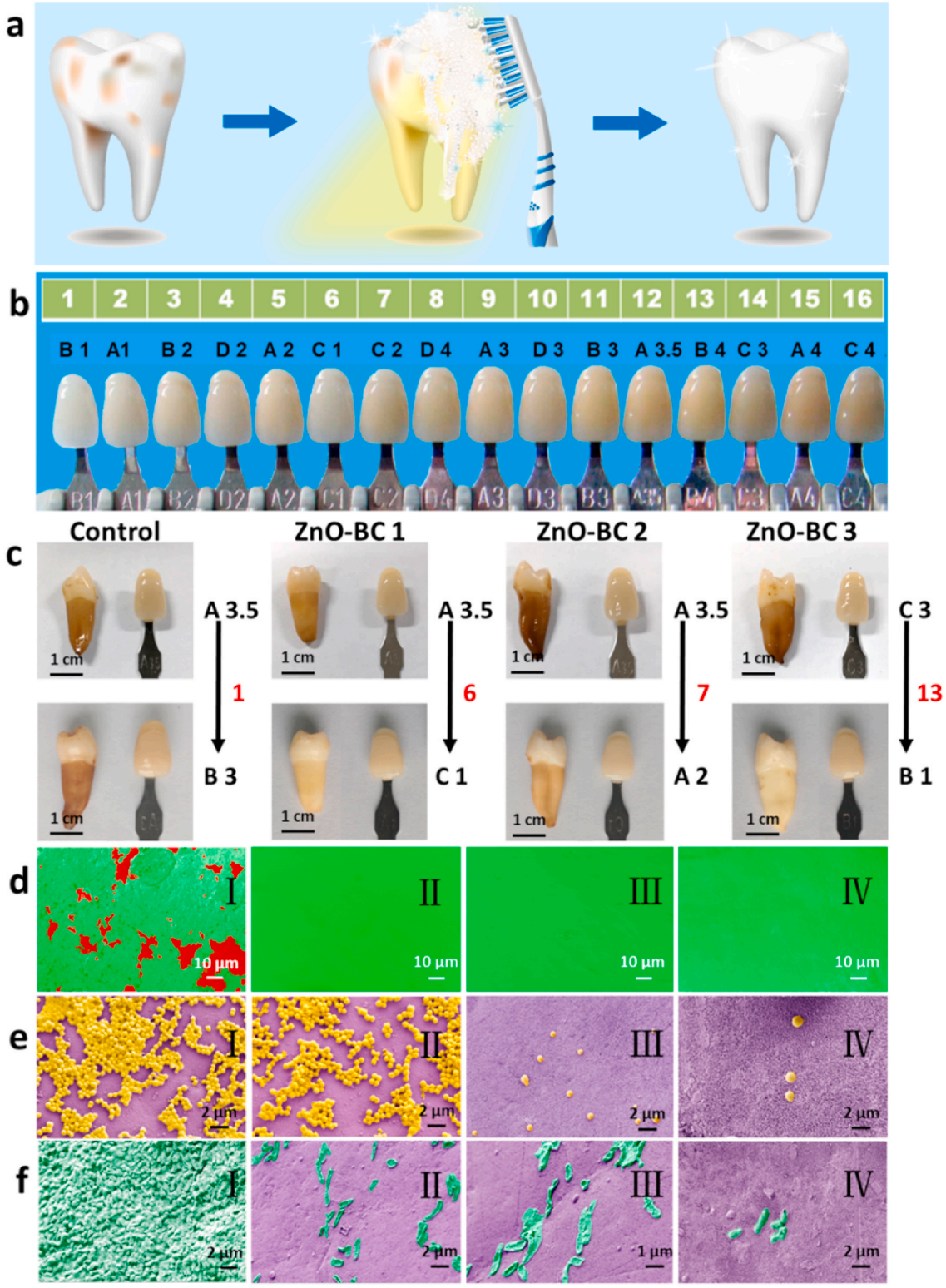

Fig. 5. Teeth whitening. (a) Schematic illustration of whitening teeth with ZnO-BC under PYLED irradiation. (b) The dental professional color card which could be used to evaluate the whitening effect. (c) Whitening effect of three kinds of ZnO-BC under PYLED irradiation. The control group was treated with tooth-paste under the same condition. (d) SEM images of tooth enamel after treatment with H_2O_2 (I), ZnO-BC 1 (II), ZnO-BC 2 (III), ZnO-BC 3 (lV). Green: normal tooth enamel, red: damaged tooth enamel. (e–f) SEM images of *S. aureus* and *E. coli* on the surface of teeth before whitening treatment (I), and after whitening treatment with ZnO-BC 1 (II), ZnO-BC 2 (III), ZnO-BC 3 (lV).

CRediT authorship contribution statement

Xinxin Miao: Conceptualization, Methodology, Software, Writing – original draft. **Fen Yu:** Data curation, Methodology, Writing – review & editing. **Kuan Liu:** Investigation, Methodology. **Zhongsheng Lv:** Formal analysis, Data curation. **Jianjian Deng:** Visualization, Software. **Tianlong Wu:** Validation. **Xinyan Cheng:** Methodology, Software. **Wei Zhang:** Methodology. **Xigao Cheng:** Supervision, Funding acquisition. **Xiaolei Wang:** Validation, Project administration, Writing – review & editing, Funding acquisition.

Declaration of competing interest

The authors declare no conflict of interest.

Acknowledgements

This work was supported by the National Natural Science Foundation of China (No. 31860263 to Xiaolei Wang); Science Foundation of Jiangxi Provincial Department of Science and Technology (20182BCB22019 to Xigao Cheng); Science Foundation of Jiangxi Provincial Department of Education (KJLD14010, 20153BCB23035, 20161ACB21002, 20165BCB19002 to Xiaolei Wang); Nanchang University Seed Grant for Biomedicine.

Appendix A. Supplementary data

Supplementary data to this article can be found online at https://doi.org/10.1016/j.bioactmat.2021.05.027.

References

[1] D. Segets, J. Gradl, R.K. Taylor, V. Vassilev, W. Peukert, Analysis of optical absorbance spectra for the determination of ZnO nanoparticle size distribution, solubility, and surface energy, ACS Nano 3 (7) (2009) 1703–1710.
[2] J. Cao, B. Wu, R. Chen, Y. Wu, Y. Hui, B.-W. Mao, N. Zheng, efficient, hysteresis-free, and stable perovskite solar cells with ZnO as electron-transport layer: effect of surface passivation, Adv. Mater. 30 (11) (2018) 1705596.
[3] Z. Kang, H. Si, S. Zhang, J. Wu, Y. Sun, Q. Liao, Z. Zhang, Y. Zhang, Interface engineering for modulation of charge carrier behavior in ZnO photoelectrochemical water splitting, Adv. Funct. Mater. 29 (15) (2019) 1808032.
[4] Z. Neščáková, K. Zheng, L. Liverani, Q. Nawaz, D. Galusková, H. Kaňková, M. Michálek, D. Galusek, A. Boccaccini, Multifunctional zinc ion doped sol-gel derived mesoporous bioactive glass nanoparticles for biomedical applications, Bioactive materials 4 (2019) 312–321.
[5] J. Yoo, Y.J. Hong, H.S. Jung, Y.J. Kim, C.H. Lee, J. Cho, Y.J. Doh, L.S. Dang, K. H. Park, G.-C. Yi, Fabrication and optical characteristics of position-controlled ZnO nanotubes and ZnO/$Zn_{0.8}M_{90.2}O$ coaxial nanotube quantum structure arrays, Adv. Funct. Mater. 19 (10) (2009) 1601–1608.
[6] G. Chen, C. Song, C. Chen, S. Gao, F. Zeng, F. Pan, Resistive switching and magnetic modulation in cobalt-doped ZnO, Adv. Mater. 24 (26) (2012) 3515–3520.
[7] Y. Yang, W. Guo, J. Qi, Y. Zhang, Flexible piezoresistive strain sensor based on single Sb-doped ZnO nanobelts, Appl. Phys. Lett. 97 (22) (2010) 223107.
[8] B. Bolhari, N. Meraji, M. Rezazadeh Sefideh, P. Pedram, Evaluation of the properties of Mineral Trioxide Aggregate mixed with Zinc Oxide exposed to different environmental conditions, Bioactive materials 5 (3) (2020) 516–521.
[9] X. Qiu, Y. Zhang, Y. Zhu, C. Long, L. Su, S. Liu, Z. Tang, Applications of nanomaterials in asymmetric photocatalysis: recent progress, challenges, and opportunities, Adv. Mater. 33 (6) (2021) 2001731.
[10] S. Kilper, S.J. Facey, Z. Burghard, B. Hauer, D. Rothenstein, J. Bill, Macroscopic properties of biomimetic ceramics are governed by the molecular recognition at the bioorganic-inorganic interface, Adv. Funct. Mater. 28 (10) (2018) 1705842.
[11] M.S. Yao, W.X. Tang, G.E. Wang, B. Nath, G. Xu, MOF thin film-coated metal oxide nanowire array: significantly improved chemiresistor sensor performance, Adv. Mater. 28 (26) (2016) 5229–5234.
[12] W.S. Lee, D. Kim, B. Park, H. Joh, H.K. Woo, Y.-K. Hong, T.-i. Kim, D.H. Ha, S. J. Oh, Multiaxial and transparent strain sensors based on synergetically reinforced and orthogonally cracked hetero-nanocrystal solids, Adv. Funct. Mater. 29 (4) (2019) 1806174.
[13] L. Wang, S. Liu, Z. Wang, Y. Zhou, Y. Qin, Z.L. Wang, Piezotronic effect enhanced photocatalysis in strained anisotropic ZnO/TiO_2 nanoplatelets via thermal stress, ACS Nano 10 (2) (2016) 2636–2643.
[14] U. Ozgur, Y.I. Alivov, C. Liu, A. Teke, M.A. Reshchikov, S. Dogan, V. Avrutin, S. J. Cho, H. Morkoc, A comprehensive review of ZnO materials and devices, J. Appl. Phys. *98* (4) (2005), 041301.
[15] Z. Xiao, X. Huang, K. Zhao, Q. Song, R. Guo, X. Zhang, S. Zhou, D. Kong, M. Wagner, K. Müllen, L. Zhi, Band structure engineering of schiff-base microporous organic polymers for enhanced visible-light photocatalytic performance, Small 15 (34) (2019) 1900244.
[16] S.H. Bae, J. Yu, T.G. Lee, S.-J. Choi, Protein food matrix-ZnO nanoparticle interactions affect protein conformation, but may not be biological responses, Int. J. Mol. Sci. 19 (12) (2018) 3926.
[17] T. Ellis, M. Chiappi, A. Garcia-Trenco, M. Al-Ejji, S. Sarkar, T.K. Georgiou, M.S. P. Shaffer, T.D. Tetley, S. Schwander, M.P. Ryan, A.E. Porter, Multimetallic microparticles increase the potency of rifampicin against intracellular mycobacterium tuberculosis, ACS Nano 12 (6) (2018) 5228–5240.
[18] Y. Wang, S. Song, J. Liu, D. Liu, H. Zhang, ZnO-functionalized upconverting nanotheranostic agent: multi-modality imaging-guided chemotherapy with on-demand drug release triggered by pH, Angew. Chem. Int. Ed. 54 (2) (2015) 536–540.
[19] M.C. Newton, S.J. Leake, R. Harder, I.K. Robinson, Three-dimensional imaging of strain in a single ZnO nanorod, Nat. Mater. 9 (2) (2010) 120–124.
[20] M.J. Cherukara, K. Sasikumar, W. Cha, B. Narayanan, S.J. Leake, E.M. Dufresne, T. Peterka, I. McNulty, H. Wen, S.K.R.S. Sankaranarayanan, R.J. Harder, Ultrafast three-dimensional X-ray imaging of deformation modes in ZnO nanocrystals, Nano Lett. 17 (2) (2017) 1102–1108.
[21] H. Liao, X. Miao, J. Ye, T. Wu, Z. Deng, C. Li, J. Jia, X. Cheng, X. Wang, Falling leaves inspired ZnO nanorods-nanoslices hierarchical structure for implant surface modification with two stage releasing features, ACS Appl. Mater. Interfaces 9 (15) (2017) 13009–13015.
[22] X. Miao, H. Liao, Z. Deng, C. Li, T. Wu, H. Zhang, M. Liu, X. Cheng, X. Wang, Dandelion" Inspired dual-layered nanoarrays with two model releasing features for the surface modification of 3d printing implants, ACS Biomater. Sci. Eng. 3 (10) (2017) 2259–2266.
[23] H.Y. Yue, S. Huang, J. Chang, C. Heo, F. Yao, S. Adhikari, F. Gunes, L.C. Liu, T. H. Lee, E.S. Oh, B. Li, J.J. Zhang, H. Ta Quang, L. Nguyen Van, Y.H. Lee, ZnO nanowire arrays on 3d hierachical graphene foam: biomarker detection of Parkinson's disease, ACS Nano 8 (2) (2014) 1639–1646.
[24] L. Guo, Y. Shi, X. Liu, Z. Han, Z. Zhao, Y. Chen, W. Xie, X. Li, Enhanced fluorescence detection of proteins using ZnO nanowires integrated inside microfluidic chips, Biosens. Bioelectron. 99 (2018) 368–374.
[25] P. Hlophe, L.C. Mahlalela, L.N. Dlamini, A composite of platelet-like orientated $BiVO_4$ fused with MIL-125(Ti): synthesis and characterization, Sci. Rep. 9 (2019) 1–12.
[26] A. Fujishima, K. Honda, Electrochemical photolysis of water at a semiconductor electrode, Nature 238 (5358) (1972) 37–38.
[27] H. Li, N. Li, M. Wang, B. Zhao, F. Long, Synthesis of novel and stable g-C_3N_4-Bi_2W_{O6} hybrid nanocomposites and their enhanced photocatalytic activity under visible light irradiation, Royal Society Open Science 5 (3) (2018) 171419.
[28] K.J. Kim, P.B. Kreider, H.G. Ahn, C.H. Chang, Characterization of cotton ball-like Au/ZnO photocatalyst synthesized in a micro-reactor, Micromachines 9 (7) (2018) 322.
[29] F. Vankuijk, Effects of ultraviolet-light on the eye - role of protective glasses, Environ. Health Perspect. 96 (1991) 177–184.
[30] G.J. Clydesdale, G.W. Dandie, H.K. Muller, Ultraviolet light induced injury: immunological and inflammatory effects, Immunol. Cell Biol. 79 (6) (2001) 547–568.
[31] F. Li, Y. Ding, P.X.X. Gao, X.Q. Xin, Z.L. Wang, Single-cystal hexagonal disks and rings of ZnO: low-temperature, large-scale synthesis and growth mechanism, Angew. Chem. Int. Ed. 43 (39) (2004) 5238–5242.
[32] S. Ma, J. Xue, Y. Zhou, Z. Zhang, X. Wu, A facile route for the preparation of ZnO/C composites with high photocatalytic activity and adsorption capacity, CrystEngComm 16 (21) (2014) 4478–4484.
[33] X. Zhang, J. Qin, Y. Xue, P. Yu, B. Zhang, L. Wang, R. Liu, Effect of aspect ratio and surface defects on the photocatalytic activity of ZnO nanorods, Sci. Rep. 4 (2014) 4549.
[34] R.J. Wurtman, The effects of light on the human body, Sci. Am. 233 (1) (1975) 69–77.
[35] I. Daou, H. Beaudry, A.R. Ase, J.S. Wieskopf, A. Ribeiro-da-Silva, J.S. Mogil, P. Seguela, Optogenetic silencing of Nav1.8-positive afferents alleviates inflammatory and neuropathic pain, eNeuro 3 (1) (2016) e0140–e0155.
[36] S. Muthu, F.J.P. Schuurmans, M.D. Pashley, Red, green, and blue LEDs for white light illumination, IEEE J. Sel. Top. Quant. Electron. 8 (2) (2002) 333–338.
[37] J. Lin, X. Ding, C. Hong, Y. Pang, L. Chen, Q. Liu, X. Zhan, H. Xin, X. Wang, Several biological benefits of the low color temperature light-emitting diodes based normal indoor lighting source, Sci. Rep. 9 (2019) 1–8.
[38] C. Peng, S. Park, F.B. de Sousa, H. Gan, S.J. Lee, W. Wang, S. Lavender, S. Pilch, J. Han, Enhanced teeth whitening by nanofluidic transport of hydrogen peroxide into enamel with electrokinetic flows, Dent. Mater. 35 (11) (2019) 1637–1643.
[39] F. Zhang, C. Wu, Z. Zhou, J. Wang, W. Bao, L. Dong, Z. Zhang, J. Ye, L. Liao, X. Wang, Blue-light-activated Nano-TiO_2@PDA for highly effective and nondestructive tooth whitening, ACS Biomater. Sci. Eng. 4 (8) (2018) 3072–3077.
[40] H.J. Cheng, Y. Geng, J. Zhao, Evaluation of the effectiveness of cold-light whitening technique on tetracycline pigmentation teeth and aged extrinsic stain teeth, Shanghai kou qiang yi xue = Shanghai journal of stomatology 27 (1) (2018) 65–67.
[41] Y. Li, X.C. Shi, W. Li, Zinc-containing hydroxyapatite enhances cold-light-activated tooth bleaching treatment in vitro, BioMed Res. Int. 10 (2017) 1–10.
[42] C. Grimm, A. Wenzel, T.P. Williams, P.O. Rol, F. Hafezi, C.E. Remé, Invest. Ophthalmol. Vis. Sci. 42 (2001) 497–505.

[43] D.S. Michaud, Z. Fu, J. Shi, M. Chung, Periodontal disease, tooth loss, and cancer risk, Epidemiol. Rev. 39 (1) (2017) 49–58.
[44] M. Stefanidou, C. Maravelias, A. Dona, C. Spiliopoulou, Zinc: a multipurpose trace element, Arch. Toxicol. 80 (1) (2006) 1–9.
[45] Y. Dai, Y. Zhang, Q.K. Li, C.W. Nan, Synthesis and optical properties of tetrapod-like zinc oxide nanorods, Chem. Phys. Lett. 358 (1–2) (2002) 83–86.
[46] Z. Yin, Duoni, H. Chen, J. Wang, W. Qian, M. Han, F. Wei, Resilient, mesoporous carbon nanotube-based strips as adsorbents of dilute organics in water, Carbon 132 (2018) 329–334.
[47] K.K. Shimabuku, A.M. Kennedy, R.E. Mulhern, R.S. Summers, Evaluating activated carbon adsorption of dissolved organic matter and micropollutants using fluorescence spectroscopy, Environ. Sci. Technol. 51 (5) (2017) 2676–2684.